Received: 29 April 2020 | Revised: 20 July 2020

DOI: 10.1111/mmi.14581

WILEY

ORIGINAL ARTICLE

Specialized and shared functions of diguanylate cyclases and phosphodiesterases in *Streptomyces* development

Julian Haist[1] | Sara Alina Neumann[1] | Mahmoud M. Al-Bassam[2] | Sandra Lindenberg[1] | Marie A. Elliot[3] | Natalia Tschowri[1]

[1]Department of Biology/Microbiology, Humboldt-Universität zu Berlin, Berlin, Germany

[2]Department of Pediatrics, University of California, San Diego, CA, USA

[3]Department of Biology, McMaster University, Hamilton, ON, Canada

Correspondence
Natalia Tschowri, Department of Biology/Microbiology, Humboldt-Universität zu Berlin, 10115 Berlin, Germany.
Email: natalia.tschowri@hu-berlin.de

Present address
Sandra Lindenberg, GlaxoSmithKline GmbH & Co. KG, Prinzregentenplatz 9:81675, München, Germany

Funding information
Natural Sciences and Engineering Council of Canada, Grant/Award Number: RGPIN-2015-04681; Deutsche Forschungsgemeinschaft, Grant/Award Number: TS 325/1-1, TS 325/2-1 and TS 325/2-2

Abstract

The second messenger bis-3,5-cyclic di-guanosine monophosphate (c-di-GMP) determines when *Streptomyces* initiate sporulation. c-di-GMP signals are integrated into the genetic differentiation network by the regulator BldD and the sigma factor σ^{WhiG}. However, functions of the development-specific diguanylate cyclases (DGCs) CdgB and CdgC, and the c-di-GMP phosphodiesterases (PDEs) RmdA and RmdB, are poorly understood. Here, we provide biochemical evidence that the GGDEF-EAL domain protein RmdB from *S. venezuelae* is a monofunctional PDE that hydrolyzes c-di-GMP to 5′pGpG. Despite having an equivalent GGDEF-EAL domain arrangement, RmdA cleaves c-di-GMP to GMP and exhibits residual DGC activity. We show that an intact EAL motif is crucial for the in vivo function of both enzymes since strains expressing protein variants with an AAA motif instead of EAL are delayed in development, similar to null mutants. Transcriptome analysis of Δ*cdgB*, Δ*cdgC*, Δ*rmdA*, and Δ*rmdB* strains revealed that the c-di-GMP specified by these enzymes has a global regulatory role, with about 20% of all *S. venezuelae* genes being differentially expressed in the *cdgC* mutant. Our data suggest that the major c-di-GMP-controlled targets determining the timing and mode of sporulation are genes involved in cell division and the production of the hydrophobic sheath that covers *Streptomyces* aerial hyphae and spores.

KEYWORDS
c-di-GMP, diguanylate cyclase, EAL, GGDEF, phosphodiesterase, *Streptomyces*

1 | INTRODUCTION

Cellular levels of the bacterial second messenger bis-3′,5′-cyclic di-guanosine monophosphate are controlled by the competing activities of GGDEF-domain containing diguanylate cyclases (DGCs) that produce the molecule out of GTP, and by phosphodiesterases (PDEs) that carry an EAL or HD-GYP domain to degrade the second messenger (Jenal *et al*., 2017). Multiplicity of c-di-GMP-turnover genes within a genome is widespread in bacteria, making it challenging to understand how individual DGCs and PDEs control specific cellular responses while sharing common enzymatic activities (Hengge, 2009). For example, *Escherichia coli* K-12 has 12 DGCs and 13 PDEs. While deleting distinct DGCs and PDEs has no effect on cellular c-di-GMP levels, it has drastic consequences for *E. coli*

Julian Haist and Sara Alina Neumann contributed equally to this work.

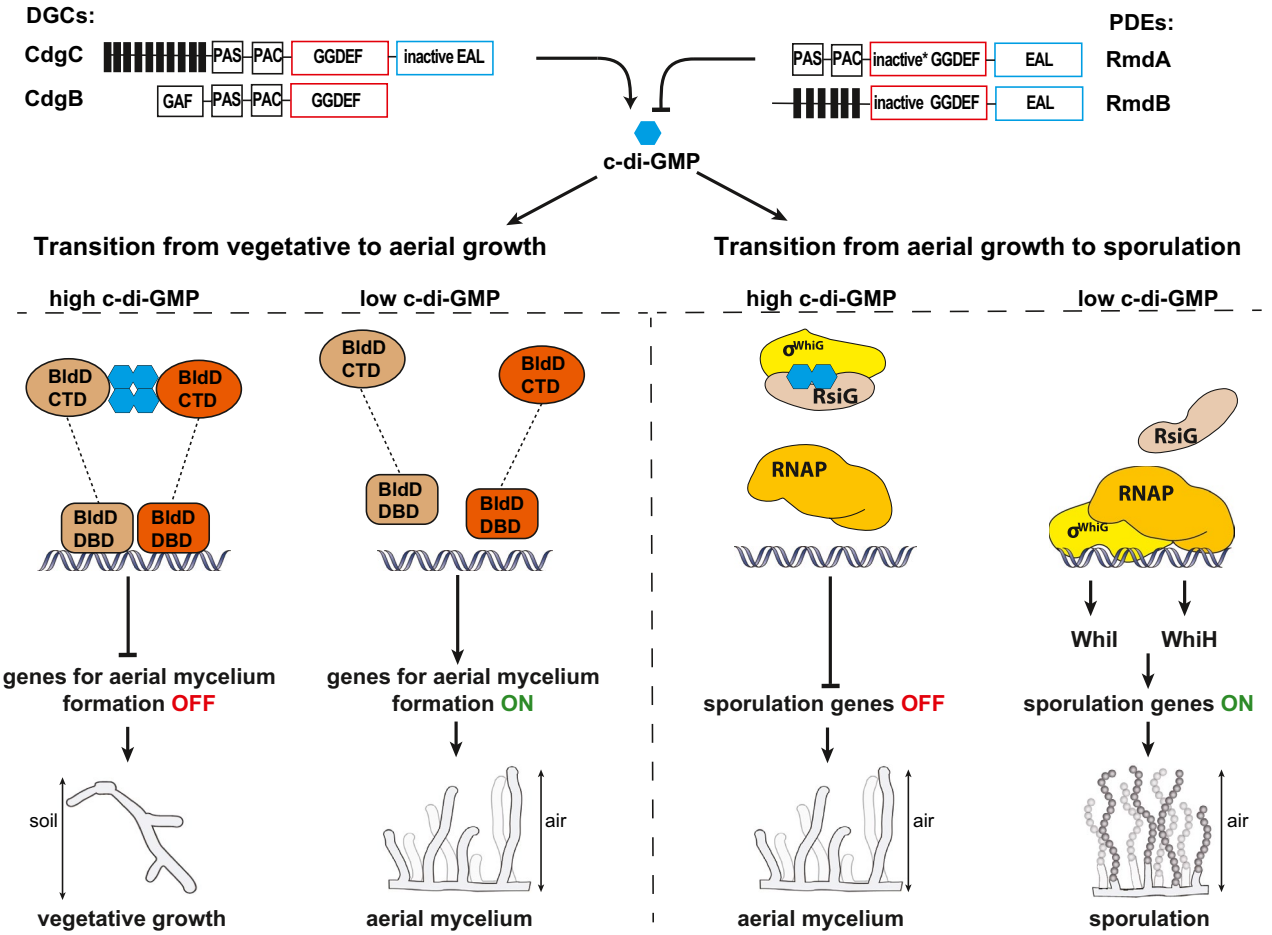

FIGURE 1 c-di-GMP signaling components in the control of *Streptomyces* development. The diguanylate cyclase (DGC) CdgC contains 10 predicted transmembrane (TM) helices (black bars), PAS-PAC signaling domains, an active GGDEF and a degenerate EAL domain that has no enzymatic activity Al-Bassam *et al*. (2018). CdgB is a soluble DGC with GAF-PAS-PAC signaling domains and an active GGDEF domain (Tran *et al*. 2011). The phosphodiesterases (PDEs) RmdA and RmdB both contain conserved GGDEF and EAL domains. Only the GGDEF domain of RmdA has residual DGC activity (indicated by (*), see Figure 2b and text). RmdA contains PAS-PAC domains for signal integration, RmdB has 6 predicted TM helices. c-di-GMP specified by CdgC, CdgB, RmdA, and RmdB controls developmental transitions via BldD and RsiG-σ^{WhiG}. BldD binds tetrameric c-di-GMP to repress transcription of genes for aerial mycelium formation, and thus, determining vegetative growth Tschowri *et al*. (2014). Dissociation of the BldD-(c-di-GMP) complex at low c-di-GMP results in derepression of BldD-targets and allows formation of aerial mycelium. During the transition from aerial growth to sporulation, the sigma factor σ^{WhiG} is kept inactive by the anti-sigma factor RsiG and c-di-GMP. Released σ^{WhiG} at low c-di-GMP activates expression of *whiI* and *whiH* that both encode developmental regulators controlling large regulons Gallagher *et al*. (2020). Activation of WhiI- and WhiH-dependent genes induces spore formation.

biofilm formation (Sarenko *et al*., 2017). In *Vibrio cholerae*, which possesses 53 proteins with c-di-GMP-metabolizing domains, only a subset of these proteins affects motility, biofilm formation, or both (Lim *et al*., 2006).

c-di-GMP is renowned for its function in guiding the transition between motility and sessility in most bacteria (Römling *et al*., 2013). High levels of the second messenger favor the switch to sessility, a process that often involves formation of self-organized, structured biofilms as a survival strategy. In the nonmotile streptomycetes, c-di-GMP is a key factor controlling the transition between their filamentous lifestyle and spore formation. However, in these bacteria, *low* levels of the molecule favor initiation of their sporulation survival strategy. For example, overexpression of the *E. coli* PDE PdeH in *S. venezuelae* induces premature, massive sporulation (Tschowri *et al*., 2014). A classical *Streptomyces* life cycle includes the erection of hyphae into the air when the bacteria switch to their stationary growth phase, followed by the morphogenesis of these aerial filaments into chains of spores. In *S. venezuelae*, aerial mycelium formation is completely bypassed when c-di-GMP levels are too low, due to PDE overexpression (Tschowri *et al*., 2014). A phenotypically identical response can be caused through deleting the DGC-encoding gene *cdgC*–one of the 10 chromosomally encoded GGDEF/EAL/HD-GYP genes in *S. venezuelae* (Al-Bassam *et al*., 2018; Latoscha *et al*., 2019). Deletion of yet another DGC-encoding gene, *cdgB*, also leads to precocious sporulation; however, the *cdgB* mutant still undergoes the classical *Streptomyces* life cycle and forms spores on reproductive aerial hyphae like the wild type. Therefore, deleting *cdgB* shifts sporulation timing but does not affect the principle mode of spore formation, that is, transition of aerial hyphae into chains of spores. Conversely, overexpressing the *S. coelicolor* DGC, CdgB,

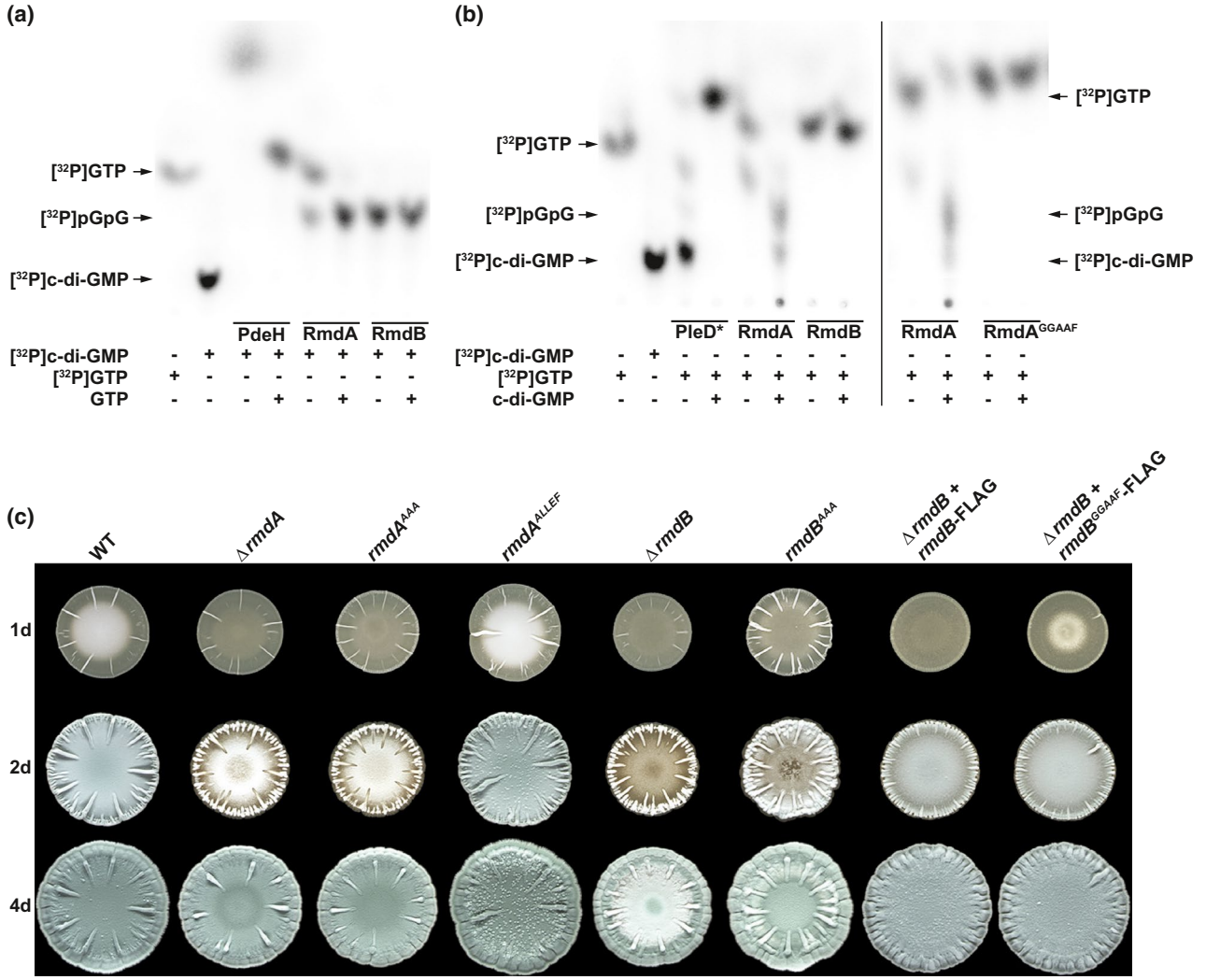

FIGURE 2 Enzymatic activities of RmdA and RmdB. Purified RmdA and RmdB were assayed for PDE activity with [^{32}P]c-di-GMP (2.08 nM) (a) and for DGC activity with [^{32}P]GTP (4.16 nM) (b) as substrate. RmdA carrying a mutagenized GGDEF motif (RmdA^{GGAAF}) was tested for DGC function in (b). Where indicated, samples also contained either 1 mM GTP or 1 mM c-di-GMP as competitors. The PDE PdeH from *E. coli* and the DGC PleD* from *C. crescentus* served as positive controls for the PDE and DGC assays, respectively. One μM of each purified protein was used in reactions. (c) Macrocolonies of *S. venezuelae* wild type and mutants were grown for up to 4 days (d) at 30°C. Development of strains carrying the mutagenized AAA motif instead of EAL in the chromosomal *rmdA* (*rmdA*^{AAA}) or *rmdB* (*rmdB*^{AAA}) and corresponding deletion mutants (Δ*rmdA* or Δ*rmdB*) was analyzed. Wild-type RmdB-FLAG and a mutant variant with the GGAAF motif instead of GGDEF (RmdB^{GGAAF}-FLAG) were expressed from the Φ_{BT1} phage integration site under the control of the native *rmdB* promoter.

causes an opposing phenotype in *S. venezuelae*, in that it prolongs filamentous, vegetative growth (Al-Bassam *et al*., 2018); this process can be mimicked by deleting either *rmdA* or *rmdB*, which encode functional PDEs (Hull *et al*., 2012).

Streptomyces development is controlled by a complex network of Bld and Whi regulators. Strains mutated in *bld* genes fail to develop aerial hyphae, while deletion of *whi* genes blocks the transition of aerial hyphae into spores (Bush *et al*., 2015). c-di-GMP signals are integrated in the two *Streptomyces* cell-fate establishing stages and determine (I) the period of vegetative, filamentous growth by binding to the transcriptional regulator, BldD, (Tschowri *et al*., 2014) and (II) initiation of sporulation by controlling the activity of the sporulation-specific sigma factor σ^{WhiG} (Figure 1) (Gallagher *et al*., 2020). Binding of c-di-GMP to BldD induces protein dimerization and stimulates BldD-binding to target DNA. In *S. venezuelae*, BldD binds to 282 target sequences in vivo and represses sporulation. Consequently, the *bldD* mutant bypasses aerial mycelium formation and sporulates precociously (Tschowri *et al*., 2014). σ^{WhiG} activity is determined by the anti-σ factor RsiG, which sequesters σ^{WhiG} when in complex with c-di-GMP. Upon release at low c-di-GMP levels, σ^{WhiG} directly activates three genes: *whiI*, *whiH*, and *vnz15005*. Through the sporulation-specific regulators WhiI and WhiH, σ^{WhiG} thus controls a large regulon of sporulation genes. Overexpressing either *whiG* or co-overexpressing *whiI* and *whiH*, induces hypersporulation (Gallagher *et al*., 2020), as seen for Δ*cdgC*.

Although direct targets of the two c-di-GMP-sensors in *Streptomyces*, BldD and σ^{WhiG}, are known, there is a major gap in our understanding of c-di-GMP-responsive genes in the genus. The

specific molecular targets driving hypersporulation in the two DGC mutants (Δ*cdgB* and Δ*cdgC*) on the one hand, and delaying sporulation in the two PDE mutants (Δ*rmdA* and Δ*rmdB*) on the other hand, are not defined. Moreover, it is unclear why the *cdgB* mutant forms premature spores within aerial hyphae, while the *cdgC* mutant is unable to raise aerial mycelium, despite their products possessing the same enzymatic function. To understand the shared, and specialized roles of the two DGCs and PDEs, respectively, we used RNA-sequencing (RNA-seq) to compare the transcriptional profiles of Δ*cdgB*, Δ*cdgC*, Δ*rmdA*, and Δ*rmdB*, with wild-type *S. venezuelae*. We found that expression of the hydrophobic sheath genes is strongly responsive to DGC and PDE deletions. Chaplin and rodlins are upregulated in Δ*cdgB*, but are downregulated in Δ*cdgC*, explaining the failure of Δ*cdgC* to raise aerial mycelium. Moreover, we show that DGCs and PDEs antagonistically control expression of cell division components, likely contributing to c-di-GMP-induced shifts in timing of sporulation initiation. The distinct regulons of the DGCs CdgB and CdgC, and of the PDEs RmdA and RmdB, imply that these enzymes orchestrate distinct cellular responses to specific environmental and metabolic signals.

2 | RESULTS AND DISCUSSION

2.1 | Biochemical and physiological activities of the GGDEF and EAL domains of RmdA and RmdB

The cytosolic RmdA and the membrane-bound RmdB are composite GGDEF-EAL domain proteins (Figure 1) that are functional PDEs in *S. coelicolor* (Hull *et al*., 2012) but their enzymatic activities have not been characterized for the *S. venezuelae* homologs. The GGDEF and the EAL domains are fully conserved in both proteins. GGDEF domains bind GTP and can allosterically modulate the activities of EAL-domains when organized in tandem, as demonstrated for the GGDEF-EAL PDE CC3396 from *Caulobacter crescentus* (Christen *et al*., 2005). We wondered whether the GGDEF domains of RmdA and RmdB were capable of GTP conversion into c-di-GMP, or if they had any influence on the activity of their associated EAL domains. We purified RmdA fused to a maltose-binding protein (MBP) tag at its N-terminus, and an N-terminally 6× His-tagged cytosolic fraction of RmdB. The PDE PdeH from *Escherichia coli* and the DGC PleD* from *C. crescentus* served as positive controls for the PDE and DGC assays, respectively (Paul *et al*., 2004; Pesavento *et al*., 2008). [^{32}P]-labeled c-di-GMP or [^{32}P]GTP was added as a substrate for in vitro PDE and DGC assays, respectively, and the reactions were separated by thin layer chromatography (TLC).

Our data show that RmdB hydrolyzed [^{32}P]c-di-GMP to the linear [^{32}P]pGpG (Figure 2a). This reaction was more efficient in presence of manganese than magnesium ions, revealing that Mn^{2+} is the preferred cofactor (Figure S1). In contrast, RmdA cleaved [^{32}P] c-di-GMP to [^{32}P]GMP via the intermediate [^{32}P]pGpG. Interestingly, excess GTP inhibited the RmdA-mediated hydrolysis of [^{32}P]pGpG to [^{32}P]GMP, suggesting that GTP binding to the GGDEF domain compromises the PDE activity of the EAL domain (Figure 2a). While EAL-domain protein-mediated hydrolysis of c-di-GMP to pGpG is considered to be physiologically relevant (Schmidt *et al*., 2005), further cleavage of pGpG to GMP, as we demonstrate here for RmdA (Figure 2a), has also been reported for PdeL, PdeR, and PdeH from *E. coli* (Schmidt *et al*., 2005; Lindenberg *et al*., 2013).

Incubation of RmdB with [^{32}P]GTP did not result in any reaction products, suggesting that the GGDEF domain is inactive, at least under the conditions tested here (Figure 2b). In contrast, we detected an additional spot after separating the reaction sample containing RmdA and [^{32}P]GTP. We hypothesized that this spot represented an intermediate product of c-di-GMP synthesis. To reduce the immediate EAL-domain-mediated hydrolysis of any [^{32}P] c-di-GMP produced by the GGDEF domain of RmdA, we added nonlabeled c-di-GMP as competitor. Indeed, we detected both [^{32}P] c-di-GMP synthesized by RmdA, and [^{32}P]pGpG that arose due to rapid degradation of [^{32}P]c-di-GMP by its EAL domain (Figure 2b). To confirm that c-di-GMP production by RmdA required an intact GGDEF site, we mutagenized the GGDEF to GGAAF motif and used purified MBP-RmdA^{GGAAF} in the DGC assays. As expected, neither c-di-GMP nor pGpG were detectable in the reaction containing the mutagenized RmdA^{GGAAF} protein (Figure 2b). Altogether, these data show that RmdB from *S. venezuelae* is a monofunctional PDE that cleaves c-di-GMP to the linear pGpG. Conversely, RmdA hydrolyzes c-di-GMP to GMP via pGpG and has weak DGC activity that likely remains cryptic, since the c-di-GMP generated by the GGDEF domain appears to be immediately hydrolyzed by the PDE activity of the EAL domain. Such residual DGC activity in tandem proteins is not uncommon and has also been reported for the GGDEF-EAL protein PdeR from *E. coli* (Lindenberg *et al*., 2013). However, we cannot exclude the possibility that, under certain conditions sensed by the PAS-PAC signaling domains, the DGC activity of RmdA becomes dominant over the PDE function.

To assess the impact of the individual GGDEF and EAL domains of RmdA and RmdB on developmental control in vivo, we generated strains carrying chromosomal mutations in either GGDEF or EAL active sites. The strain expressing *rmdA* with an AAA motif instead of the EAL motif (*rmdA*^{AAA}) showed a delay in development, similar to that of the *rmdA* null mutant (Figure 2c). In contrast, mutagenizing the GGDEF motif to ALLEF in the chromosomal locus of *rmdA* (*rmdA*^{ALLEF}) had no effect on differentiation compared to wild type (Figure 2c). Similarly, a strain carrying the mutant AAA motif (in place of the EAL motif) in the EAL domain of *rmdB* (*rmdB*^{AAA}) was delayed in development, like the *rmdB* null mutant. We were unable to generate a strain expressing the *rmdB*^{ALLEF} allele from the chromosome, so instead we applied complementation analysis. We found that an *rmdB* allele carrying the mutagenized GGAAF motif in the GGDEF site could complement the differentiation defect of the *rmdB* mutant (Figure 2c). These data suggest that a functional EAL domain is crucial for the in vivo functions of RmdA and RmdB. While the GGDEF domain of RmdA can synthesize c-di-GMP in vitro, this activity does not seem to contribute to differentiation control by RmdA in vivo under the conditions tested.

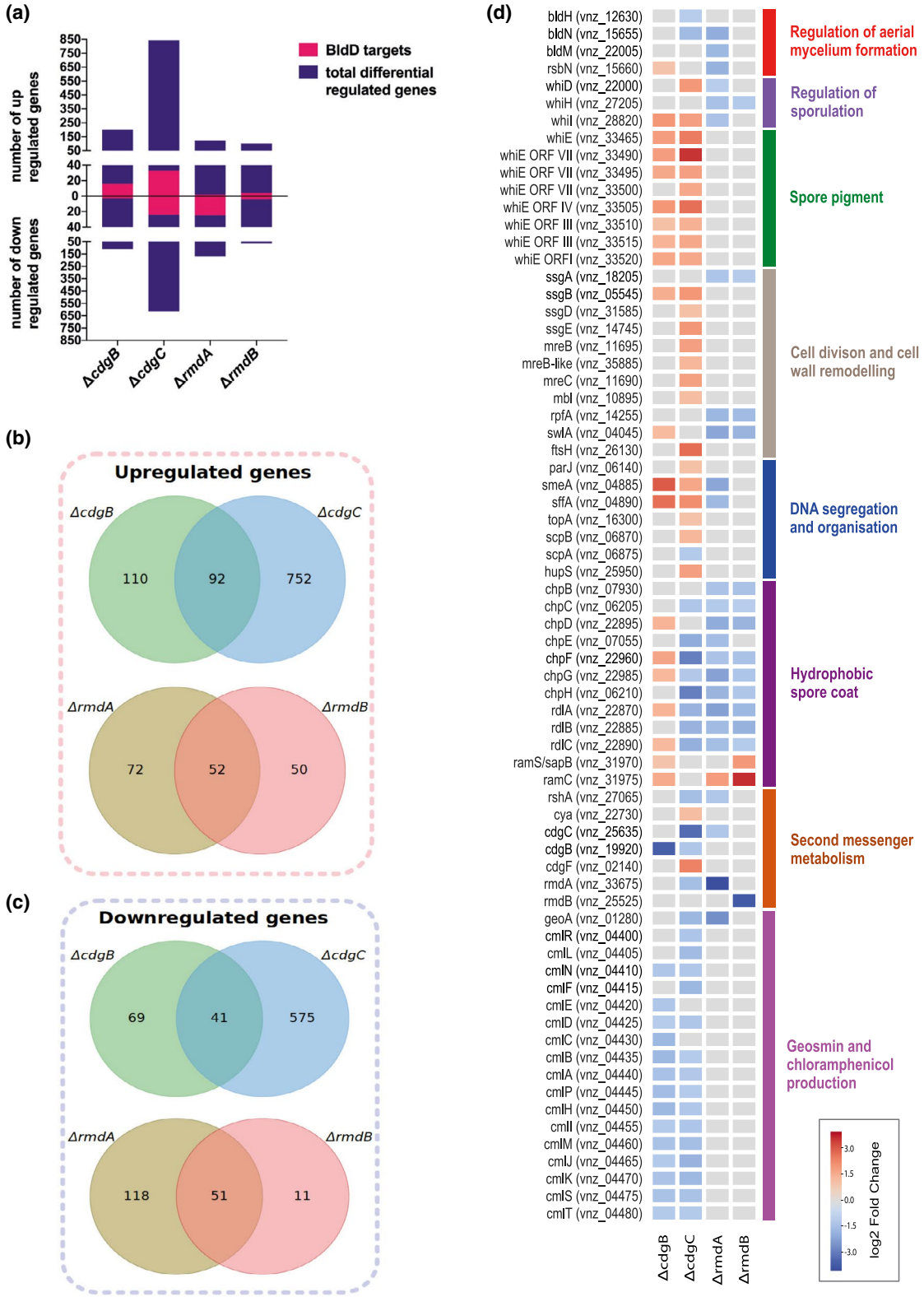

FIGURE 3 RNA-seq profiles of Δ*cdgB*, Δ*cdgC*, Δ*rmdA*, and Δ*rmdB* strains. (a) Histogram showing total numbers of down- and upregulated genes in the analyzed mutants. Out of these, numbers of differentially expressed direct BldD-targets in each strain are visualized in pink. Venn diagrams depict number of upregulated (b) and downregulated (c) genes that overlap between the two DGC mutants Δ*cdgC* and Δ*cdgB*, or between the two PDE mutants Δ*rmdA* and Δ*rmdB*. (d) Heat map showing differentially expressed genes associated with developmental processes. Genes with twofold (log2 > 1/<−1; $p_{adj} < .05$) change in expression were considered as significant

2.2 | Genome-wide transcriptional profiling of *S. venezuelae* c-di-GMP mutants

Control of developmental progression is the key function of c-di-GMP in all tested *Streptomyces* models (Tran *et al*., 2011; Tschowri *et al*., 2014; Makitrynskyy *et al*., 2020; Yan *et al*., 2020). Nevertheless, targets of the second messenger have not yet been addressed on a genome-wide scale. Out of the 10 GGDEF/EAL/HD-GYP-proteins encoded by *S. venezuelae*, only four enzymes control c-di-GMP-mediated differentiation processes. Deleting the DGC-encoding *cdgB* and *cdgC* causes precocious sporulation, but, the phenotypes of the two mutants differ, in that the Δ*cdgB* strain forms spores on aerial hyphae, whereas the Δ*cdgC* strain completely skips the aerial mycelium formation stage. On the contrary, deleting either the PDE-encoding *rmdA* or *rmdB* delays development. However, the phenotypes of these two strains are not identical: losing *rmdB* arrests *S. venezuelae* in the vegetative growth phase for ca. 1 day longer than deleting *rmdA* (Al-Bassam *et al*., 2018). These phenotypes suggest that the two DGCs and PDEs not only share common functions, but also play unique roles in developmental regulation. To understand their functions, we conducted RNA-sequencing (RNA-seq) of the transcriptomes of the four mutants and their wild-type parent strain. When cultivated in liquid Maltose-Yeast Extract-Malt Extract (MYM) medium, Δ*cdgB*, Δ*cdgC*, Δ*rmdA*, and Δ*rmdB* mutants did not show a significant difference in growth rate in comparison to the wild type (Figure S2b). However, the distinct phenotypes of the mutants were particularly pronounced when *S. venezuelae* was grown on MYM agar. Hence, for the RNA-seq analyses, we harvested macrocolonies from plates that were inoculated with identical numbers of spores (12 μl of 2×10^5 CFU/μl) and were grown for 30 h at 30°C. For each strain, three independent macrocolonies were pooled for RNA-isolation and two samples were sequenced per strain. Thus, the resulting transcriptional profiles would be representative of six (combined) biological replicates.

We were specifically interested in genes that are known components of cascades controlling differentiation (Bush *et al*., 2015); however, a complete table of differentially expressed genes is presented in Dataset S1. To reduce the complexity of interpreting the RNA-seq data, we considered genes that exhibited a more than two-fold ($\log2 > 1/<-1$; $p_{adj} < 0.05$) increase or decrease in expression in the mutants relative to the wild type as significant. Impressively, in the *cdgC* mutant, 1,458 genes exhibited significant changes in transcription, with 844 genes being up- and 616 downregulated in comparison to the wild type (Figure 3a, Dataset S1). In Δ*cdgB*, Δ*rmdA*, and Δ*rmdB*, 312, 293, and 164 genes, respectively, were differentially expressed (Figure 3a). We conclude that c-di-GMP controlled by CdgB, CdgC, RmdA, and RmdB has a global regulatory role. However, at the time of harvest, wild type, Δ*rmdA* and Δ*rmdB* were in a vegetative stage of growth, while Δ*cdgB* and Δ*cdgC* had already sporulated (Figure S2a). Therefore, we cannot exclude that some of the transcriptional changes may be indirect and result rather from differences in developmental stages between the strains than from changes in c-di-GMP.

By comparing the transcriptomes of Δ*cdgB* and Δ*cdgC*, we found only 92 upregulated and 41 downregulated genes that were shared in the two DGC mutants (Figure 3b,c). Thus, out of the 1,770 genes that are in sum differentially expressed in the two mutants, only ~8% of genes overlapped. When examining the transcription profiles of the Δ*rmdA* and Δ*rmdB* mutants, we found 52 upregulated genes and 51 downregulated genes that were common to both strains (Figure 3b,c). In total, this corresponds to ~23% of all differentially expressed genes being similarly impacted by both RmdA and RmdB. This shows that despite a shared enzymatic activity, the DGCs and the PDEs, respectively, control characteristic sets of genes. The N-termini of CdgC and RmdB are anchored in the cell membrane, CdgB has GAF-PAS-PAC N-terminal sensory domains and RmdA contains PAS-PAC domains at the N-terminus (Figure 1) (Latoscha *et al*., 2019). Likely, the signals perceived by the characteristic sensory domains specify the distinct functions of CdgB, CdgC, RmdA, and RmdB.

2.3 | *bld* and *whi* genes with altered expression in the DGC/PDE mutants

Proteins of the Bld and Whi families are key regulators of the developmental genetic network. BldD sits on top of the developmental regulatory cascade, and when in complex with c-di-GMP, it binds to 282 target promoters in the *S. venezuelae* chromosome (Tschowri *et al*., 2014; Bush *et al*., 2015). BldD acts as a transcriptional repressor on most target promoters (Elliot *et al*., 2001; den Hengst *et al*., 2010), but it can also activate gene expression (Yan *et al*., 2020). Unexpectedly, we found few *bld* and *whi* genes to be differentially expressed in the studied mutants. In agreement with a delay in development, *bldN*, *bldM*, *whiD*, *whiH*, and *whiI* were downregulated in Δ*rmdA*; however, of these, only *whiH* was also downregulated in Δ*rmdB*. In Δ*cdgB*, only *whiI* was upregulated at the tested time-point, while in Δ*cdgC*, both *whiI* and *whiD* were upregulated, while *bldH* and *bldN* were downregulated (Figure 3d and S3a).

The expression of *whiI* and *whiH* is directly activated by the sigma factor σ^{WhiG}, whose activity is controlled by the RsiG-(c-di-GMP) anti-sigma factor. Expression of *whiI* completely depends on *whiG*, whereas *whiH* expression is only partially dependent on the sigma factor (Gallagher *et al*., 2020). Thus, the fact that *whiI* was upregulated in both Δ*cdgB* and Δ*cdgC*, reflected the activation of σ^{WhiG} in the two DGC mutants. *whiH* and *whiI* were, however, both downregulated in Δ*rmdA*; *whiH* was also less expressed in Δ*rmdB*. This collectively suggests reduced activity of σ^{WhiG} in the two PDE mutant strains. The inversely correlated transcription profiles of these σ^{WhiG}-dependent genes imply that the two DGCs and two PDEs all contribute to modulating σ^{WhiG}-activity.

The BldN ECF sigma factor activates the expression of the chaplin and rodlin genes, which encode the hydrophobic sheath proteins that encase aerial hyphae and spores (Bibb *et al*., 2012). BldD-(c-di-GMP) directly represses *bldN* expression (Schumacher *et al*., 2017) (Elliot *et al*., 2001; Yan *et al*., 2020). Thus, we expected increased

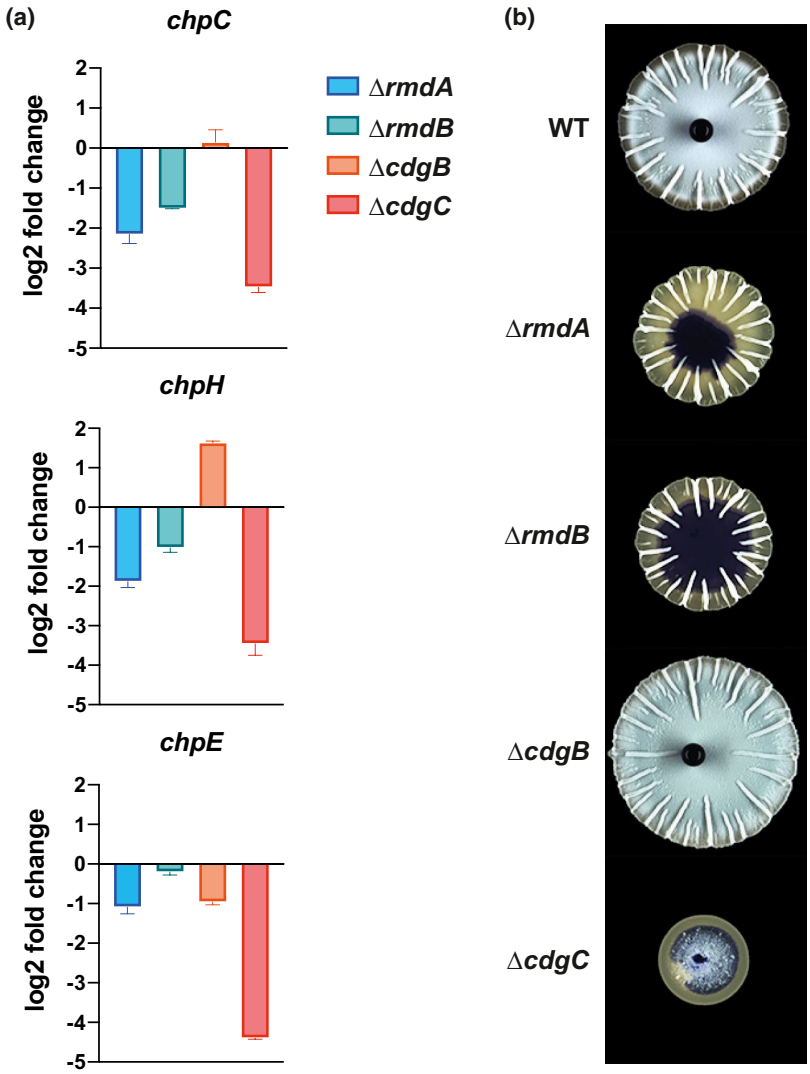

FIGURE 4 Chaplin expression in the PDE/DGC mutants and properties of their colony surfaces. (a) Strains were grown on MYM plates for 30 h at 30°C when harvested for RNA isolation that was used for qRT-PCR analysis. The assay was reproduced at least three times with three technical replicates per experiment. Expression values were calculated relative to the accumulation of the constitutively expressed *hrdB* reference mRNA and normalized to the wild-type value. log2 change > 1/<−1 was considered as significant. Data are presented as mean of technical replicates ± standard deviation (n = 3). (b) Twelve µl of $2x10^5$ CFU/µl *S. venezuelae* spores were spotted on MYM agar and incubated for 43 h at 30°C. Five µl of stained water was pipetted on top of the macrocolonies and images were taken using a binocular camera (Zeiss).

transcription of *bldN* in the DGC mutants, due to loss of BldD repressive activities, and reduced expression of *bldN* in the PDE mutants. It was, therefore, a surprise that *bldN* expression was downregulated in the Δ*cdgC* strain. Because of that we set out to examine the expression patterns of all known BldD-(c-di-GMP) target genes in our different mutants. Of the 282 direct BldD-(c-di-GMP) targets in *S. venezuelae*, we found 19, 57, 27, and 8 genes to be differentially expressed in Δ*cdgB*, Δ*cdgC*, Δ*rmdA*, and Δ*rmdB*, respectively (Figure 3a).

These analyses revealed that, at least under the conditions tested, only a relatively minor fraction of all BldD-(c-di-GMP)-targets responded to c-di-GMP changes in the studied mutants. Notably, the direct BldD-regulon was determined in *S. venezuelae* grown in liquid culture, and some of the observed differences may be explained by the fact that here, colonies grown on solid medium were analyzed. However, many direct BldD-targets are co-regulated by multiple transcription factors in a hierarchical manner (Bush *et al.*, 2015), and thus, require multiple, additional signals for proper expression. For example, in *S. venezuelae*, the response regulator MtrA, binds directly to a number of *bld* and *whi* genes that are also direct BldD-targets, including *bldM*, *bldN*, and *whiG* (Som *et al.*, 2017). MtrA acts as both activator and repressor in other actinomycetes, but how it impacts *bld* and *whi* gene expression remains to be addressed in *S. venezuelae*. Another example is the MerR-like regulator, BldC, which binds to a number of promoters that are also direct targets of BldD; like MtrA, BldC can have both repressor and activator functions (Schumacher *et al.*, 2018b).

2.4 | Hydrophobic spore coat genes are sensitive to c-di-GMP

The chaplin and rodlin proteins are major components of the hydrophobic sheath that covers the aerial hyphae and spores in *Streptomyces* (Claessen *et al.*, 2003; Elliot *et al.*, 2003). *S. venezuelae* secretes two long (ChpB and ChpC) and five short (ChpD-H) chaplins, and these proteins are expected to self-assemble into amyloid-like filaments on the cell surface, where they then permit the aerial hyphae to escape the surface tension. As further components of the hydrophobic layer, *S. venezuelae* produces three rodlin proteins

(RdlA-C), which are proposed to organize the chaplin filaments into so-called rodlets. Unlike the chaplins, however, the rodlins are dispensable for aerial development and surface hydrophobicity (Claessen *et al*., 2002). Moreover, when grown on rich medium, *Streptomyces* secrete an additional surfactant peptide, SapB (product of the *ramCSAB* operon) (Willey *et al*., 1991).

Expression of genes encoding the different hydrophobic sheath components was significantly affected in the four tested mutants. As shown using RNA-seq, deleting *cdgB* resulted in upregulation of *chpD*, *chpF*, *chpG*, *rdlA*, *rdlC*, *ramS*, and *ramC* (Figure 3d). In addition, quantitative RT-PCR (qRT-PCR) data revealed that *chpH* was also upregulated in a *cdgB* mutant (Figure 4a). Surprisingly, our data showed that in contrast to Δ*cdgB*, all chaplin genes (except *chpB and chpD),* and the three rodlin genes, *rdlA-C*, were downregulated in the *cdgC* mutant (Figure 3d), despite this strain having the same rapid sporulation phenotype as the *cdgB* mutant. qRT-PCR data confirmed that expression of *chpC*, *chpE*, and *chpH* was 11-fold, 21-fold, and 11-fold, respectively, lower in Δ*cdgC* than in wild type (Figure 4a). We also detected a strong downregulation of the chaplin and rodlin genes in both Δ*rmdA* and Δ*rmdB* strains (Figures 3d and 4a).

We tested the water repellent properties of the colony surface of the different wild-type and mutant strains, and found that wild type and Δ*cdgB* both repelled aqueous solutions (seen as pearl droplet formation on the colony surface), suggesting that they possessed a hydrophobic layer atop their colonies. In contrast, Δ*rmdA*, Δ*rmdB*, and Δ*cdgC* colonies were highly hydrophilic, with water droplets immediately dispersing (Figure 4b). The observed properties associated with these colony surfaces are consistent with expression of *chp* genes in wild type and Δ*cdgB*, and reduced expression of the chaplin genes in Δ*cdgC*, Δ*rmdA*, and Δ*rmdB*.

We wondered whether chaplin overexpression could restore the inability of Δ*cdgC*, Δ*rmdA*, and Δ*rmdB* to form aerial mycelium. To test this, we introduced *chpB-F* and *chpH*, under the control of the constitutive *ermE** promoter, on the integrative pMS82 vector into each mutant strain. Colony morphology analysis revealed that none of the overexpressed chaplin genes could fully restore aerial mycelium formation to the studied mutants, when overexpressed individually (Figure S4). Presumably, fine-tuned expression of multiple *chp* genes is needed to overcome this developmental defect (Di Berardo *et al*., 2008).

In conclusion, our data revealed that production of the amyloid-forming chaplin and rodlin proteins is controlled by c-di-GMP in *S. venezuelae*. This is reminiscent of many bacteria, in which the synthesis of extracellular matrix components is activated by c-di-GMP. For example, in *E. coli*, expression of *csgA* and *csgB*, encoding the main components of the amyloid curli fibers, is activated by c-di-GMP (Pesavento *et al*., 2008). However, strikingly, *chp* and *rdl* genes are downregulated upon deletion of the DGC *cdgC*, while deletion of the DGC *cdgB* has the opposite effects, leading to upregulation of these genes. The contrasting expression profile of these genes in the two DGC mutants explains the morphological difference between them. Obviously, lack of a hydrophobic layer means Δ*cdgC* is unable to break the surface tension at the air-agar interface and raise aerial hyphae, so that instead the spores are formed on the upper layer of the substrate mycelium. The downregulation of *chp* and *rdl* genes in Δ*cdgC* is likely a result of *bldN* downregulation in this strain (Figures 3d and S3a), where *bldN* encodes an ECF sigma factor needed for expression of these genes. *bldN* expression is governed by BldD-(c-di-GMP), while BldN activity is controlled by the membrane-bound anti-sigma factor, RsbN (Schumacher *et al*., 2018a). Since CdgC is associated with the membrane via its transmembrane helices, it will be interesting to test whether this enzyme affects *chp* and *rdl* expression through its modulation of RsbN activity.

2.5 | Cell division genes are upregulated in the DGC mutants and downregulated in the PDE mutant strains

Our RNA-seq data showed that multiple genes encoding components of the cell division, cell wall synthesis and chromosome segregation machineries, were upregulated upon deletion of *cdgC* (Figure 3d). Among these targets were *ssgB*, whose product is important for the assembly of FtsZ rings at cell division sites (Willemse *et al*., 2011); *ssgD*, encoding a protein that appears to be involved in lateral cell wall synthesis; and *ssgE*, whose product was proposed to control the correct timing of spore dissociation (Noens *et al*., 2005). In addition, the three *Streptomyces mreB*-like genes (*mreB*, *vnz35885*, and *mbl*) and *mreC* were upregulated in Δ*cdgC* (Figure 3d). MreB, Mbl, and MreC have crucial roles in the synthesis of a thickened spore wall and contribute to resistance of spores to various stresses such as heat, detergents and salt stress (Heichlinger *et al*., 2011; Kleinschnitz *et al*., 2011). The *smeA-sffA* operon, which encodes SffA, a putative DNA translocase that participates in chromosome segregation into spores, and the membrane protein SmeA, which localizes SffA to sporulation septa (Ausmees *et al*., 2007), was highly upregulated in Δ*cdgB* and Δ*cdgC* and downregulated in Δ*rmdA* (Figure 3d).

Differentiation of *Streptomyces* hyphae into spores requires the conserved tubulin-like GTPase FtsZ, which polymerizes into filaments, called Z-rings, close to the membrane and recruits additional cell division proteins (Jakimowicz & van Wezel, 2012; Haeusser & Margolin, 2016). Ladder-like array of multiple FtsZ rings define the future sporulation septa. In *S. coelicolor*, *ftsZ* expression is controlled by three promoters (Flärdh *et al*., 2000); the same organization was observed for the *ftsZ* promoter region in *S. venezuelae* (Figure 5a). The onset of sporulation coincides with a strong upregulation of *ftsZ* transcription, and this increased expression is crucial for sporulation septation (Flärdh *et al*., 2000). We expected to detect increased *ftsZ* transcript levels in the *cdgB* and *cdgC* mutants that sporulate precociously, but RNA-seq did not reveal significant changes in *ftsZ* expression in any of the mutants. Since the two DGC mutant strains have already formed spores when harvested for RNA-isolation from plates after 30 h of growth, we suspected that harvesting at an earlier time point may have revealed changes in *ftsZ* transcript levels.

Given this, we sought to address *ftsZ* expression in our mutant strains using an alternative approach. We introduced an *ftsZ-ypet*

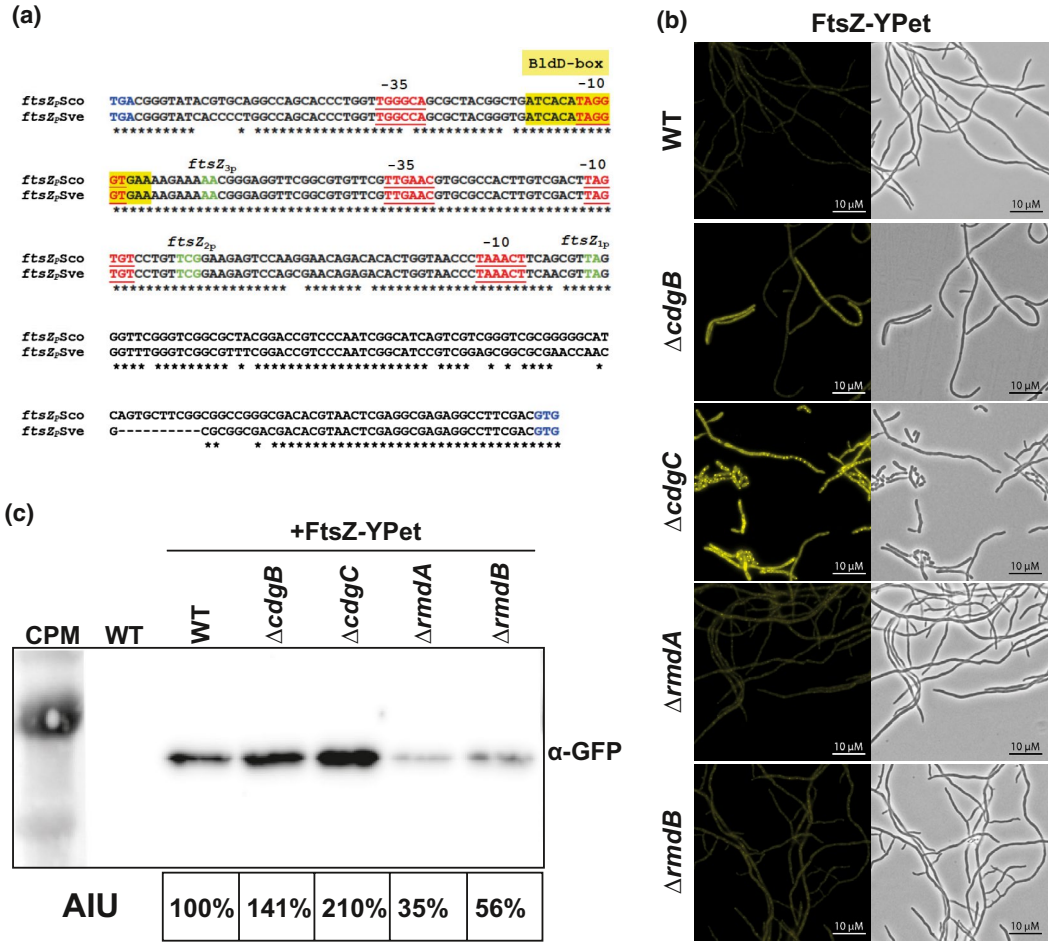

FIGURE 5 *ftsZ* expression in the *cdgB*, *cdgC*, *rmdA*, and *rmdB* mutants. (a) *ftsZ* promoter region from *S. coelicolor* ($ftsZ_P$Sco) and *S. venezuelae* ($ftsZ_P$Sve). The TGA stop codon from *ftsQ* and the GTG start codon from *ftsZ* are shown in blue. Three *ftsZ* mRNA 5´ends were mapped in the study by Flärdh *et al.* (2000) and are highlighted in green ($ftsZ_{1P}$, $ftsZ_{2P}$, and $ftsZ_{3P}$). Putative −10 and −35 promoter regions are underlined and marked in red. BldD-binding site was determined by den Hengst *et al.* (2010) in *S. coelicolor* and is fully conserved in *S. venezuelae* (yellow box). (b) Fluorescence (left) and phase contrast microscopy images (right) showing that FtsZ-YPet is upregulated in Δ*cdgB* and Δ*cdgC* after 12 h of growth in liquid MYM. FtsZ-YPet was expressed from the Φ_{BT1} integration site under control of the native *ftsZ* promoter from the pSS5 vector Schlimpert *et al.* (2017). (c) Immunoblot analysis using anti-GFP antibody for FtsZ-YPet detection. Strains were grown for 12 h in liquid MYM. Fourteen μg of total protein was loaded per lane (see Figure S5 for loading control). WT free of the FtsZ-YPet fusion was used as negative control. For quantification, arbitrary units (AIU) were determined using ImageQuantTL. CPM: color prestained protein marker (NEB)

translational fusion, under the control of the native *ftsZ* promoter on the pSS5 plasmid (Schlimpert *et al.*, 2017), into the Φ_{BT1} phage integration site in the wild-type strain, alongside the *cdgB*, *cdgC*, *rmdA*, and *rmdB* mutants. After 12 h of growth in liquid MYM medium, wild type and the two PDE mutant strains grew vegetatively and only weak FtsZ-YPet signals were detected. In contrast, in the two DGC mutants, the *ftsZ*::*ypet* fusion was highly upregulated, with abundant Z-ring ladders observed, signaling the initiation of sporulation septation. In Δ*cdgC*, single spores were already detectable at this early stage of growth (Figure 5b). Immunoblot analysis using an anti-GFP antibody confirmed that FtsZ::YPet was most abundant in Δ*cdgC*, and was elevated in Δ*cdgB* relative to the wild-type. In contrast, in Δ*rmdA* and Δ*rmdB*, FtsZ::YPet levels were strongly reduced when compared with wild-type levels (Figure 5c).

BldD integrates c-di-GMP signals into *ftsZ* transcriptional control since BldD-(c-di-GMP) directly binds to the *S. venezuelae ftsZ* promoter region, as detected using ChIP-seq analysis (Tschowri *et al.*, 2014). The BldD-binding site in the *ftsZ* promoter was defined in *S. coelicolor* (den Hengst *et al.*, 2010) and is fully conserved in *S. venezuelae* (Figure 5a). It is likely that deletion of either *cdgB* or *cdgC* leads to dissociation of the BldD repressor from the *ftsZ* promoter, while deletion of *rmdA* or *rmdB* results in prolonged BldD-(c-di-GMP)-mediated repression. In addition, *ftsZ* expression responds to c-di-GMP changes via σ^{WhiG}, which is kept inactive by RsiG-(c-di-GMP) when c-di-GMP levels are high. As demonstrated in *S. coelicolor*, deleting *whiG* or one of the two σ^{WhiG}-dependent genes, *whiI* and *whiH*, reduced or eliminated the developmental increase in *ftsZ* transcript levels (Flärdh *et al.*, 2000). Altogether, *ftsZ* expression represents a powerful c-di-GMP-sensitive reporter in *Streptomyces*, responding to both, BldD-mediated c-di-GMP-signaling during vegetative growth, and to RsiG-σ^{WhiG}-sensed c-di-GMP stimuli during the transition to sporulation.

2.6 | Genes encoding second messenger enzymes with altered expression in the DGC/PDE mutants

In vivo ChIP-seq analysis identified *cdgA*, *cdgB*, *cdgC*, and *cdgE* as direct BldD-(c-di-GMP) targets in *S. venezuelae* (Tschowri *et al*., 2014). For *cdgB*, this finding was confirmed biochemically using EMSAs (Schumacher *et al*., 2017), but such confirmation had not been performed for *cdgA*, *cdgC*, and *cdgE*. We systematically tested binding of BldD to promoters of all genes coding for c-di-GMP-metabolizing enzymes in *S. venezuelae* using EMSAs. Our in vitro data confirmed that BldD bound in a c-di-GMP-responsive manner to the promoter regions of *cdgA*, *cdgC*, and *cdgE* (Figure 6a), but we did not detect any protein binding to the promoters of *cdgD*, *cdgF*, *rmdA*, *rmdB*, and *hdgAB* (data not shown). BldD binds to a pseudo-palindromic

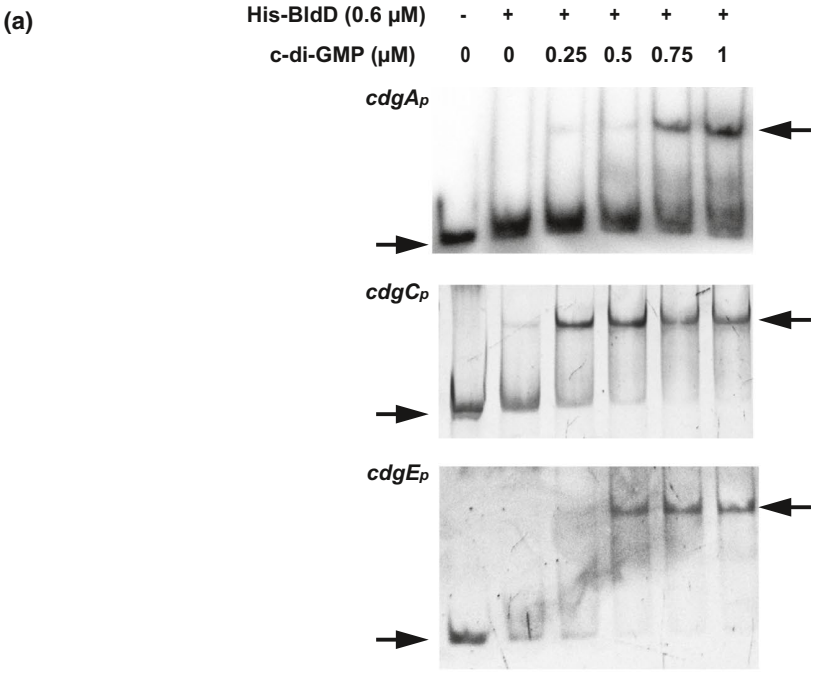

FIGURE 6 *cdgA*, *cdgC*, and *cdgE* are direct BldD targets. (a) EMSA analysis of BldD binding to *cdgA*, *cdgC*, and *cdgE* promoter DNA ± c-di-GMP (0.25–1 μM). (b) Putative BldD-binding box in the promoter regions of *cdgA*, *cdgC*, and *cdgE*. DNA consensus motif bound by BldD was determined by den Hengst *et al*. (2010) and is located 215 bp upstream of the GTG start in $cdgA_P$, 224 bp upstream of the GTG start in $cdgC_P$ and 59 bp upstream of the ATG start in $cdgE_P$. (C) Enzyme assay shows that CdgE is an active DGC and that nonlabeled c-di-GMP inhibits CdgE-mediated conversion of [^{32}P]GTP into [^{32}P]c-di-GMP. The DGC PleD* from *C. crescentus* served as positive control. Co: [^{32}P]GTP control

sequence, designated the BldD box; such boxes were located 215, 224, and 59 bp upstream of the translational start codons of *cdgA*, *cdgC*, and *cdgE*, respectively (Figure 6b). CdgA, CdgB, and CdgC are active DGCs (den Hengst *et al*., 2010; Tran *et al*., 2011; Al-Bassam *et al*., 2018). We sought to test the DGC activity for CdgE (possessing GAF-GGDEF domains), and found that indeed it too had DGC activity (Figure 6c). Intriguingly, CdgE activity was subject to product inhibition, since added nonlabeled c-di-GMP inhibited conversion of [^{32}P]GTP into [^{32}P]c-di-GMP (Figure 6c).

This regulatory feedback loop comprising BldD as c-di-GMP sensor that controls expression of four active DGCs let us hypothesize that expression of *cdgA*, *cdgB*, *cdgC*, and *cdgE* may be altered in the analyzed DGC/ PDE mutant strains. However, according to RNA-seq, neither transcript abundance of *cdgA*, nor that of *cdgE*, was affected at the tested time point in any of the mutants (Figure 3d). *cdgC* expression was reduced upon *rmdA* deletion, while *cdgB* transcript levels were lower in Δ*cdgC* than in wild type (Figure 3d and S3b). Deleting *cdgC* also resulted in downregulation of *rmdA* and upregulation of *cdgF* (Figure 3d and S3b), which codes for a PAS-PAC-GGDEF-EAL protein that contains 10 predicted transmembrane helices (Latoscha *et al*., 2019).

Transcriptional regulation of c-di-GMP-metabolizing enzymes in *S. venezuelae* is complex and involves the action of multiple global regulators, likely explaining why BldD activity modulation due to changes in c-di-GMP levels in the tested DGC/ PDE mutants was not associated with significant transcriptional changes in these genes, at least under the studied conditions. The four direct BldD-(c-di-GMP) targets (*cdgA*, *cdgB*, *cdgC*, and *cdgE*) are also directly controlled by the response regulator MtrA, which further binds to the promoters of *cdgF* and *rmdB* (Som *et al*., 2017). Moreover, *cdgB* is directly repressed by the transcription factor WhiA, while *cdgE* is directly activated by the MerR-like regulator BldC (Bush *et al*., 2013, Bush *et al*., 2019). Such multilayered transcriptional control of c-di-GMP synthesis and degradation suggests that levels of this molecule are fine-tuned in response to disparate signal transduction cascades.

Differential expression of c-di-GMP-metabolizing enzymes in the analyzed mutants and the regulatory feedback loop comprising BldD-(c-di-GMP) and the four active DGCs CdgA, CdgB, CdgC, and CdgE let us question the c-di-GMP levels in Δ*cdgC*, Δ*cdgB*, Δ*rmdA*, and Δ*rmdB*. We determined intracellular c-di-GMP levels in cell extracts using liquid chromatography tandem mass spectrometry (LC-MS/MS) (see extended experimental procedures in the supplementary information) and detected ~ twofold elevated levels of the second messenger in the four mutants when compared to wild-type levels (Figure S2c). Increased c-di-GMP in Δ*rmdA* and Δ*rmdB* is not surprising, but is unexpected for Δ*cdgB* and Δ*cdgC* and shows that levels of c-di-GMP do not correlate with the opposing sporulation phenotypes of the PDE and DGC mutants. In *E. coli*, global c-di-GMP levels do not correlate with biofilm formation phenotype since local c-di-GMP-signaling mechanisms control the synthesis of curli fibers and of pEtN-cellulose (Sarenko *et al*., 2017) (Richter *et al*., 2020). Thus, it is likely that locally acting c-di-GMP is also involved in regulation of *Streptomyces* sporulation.

In addition to genes coding for c-di-GMP-turnover enzymes, we found that *rshA*, encoding a RelA/SpoT homolog containing a conserved HD-domain for hydrolysis of the alarmone (p)ppGpp (Latoscha *et al*., 2019) was downregulated in Δ*cdgC* and Δ*rmdA* (Figure 3d). Moreover, *cya*, encoding a cAMP synthetase was upregulated in Δ*cdgC*, suggesting that CdgC links c-di-GMP-signaling to (p)ppGpp and cAMP metabolism.

2.7 | Natural product genes differentially expressed in Δ*cdgB* and Δ*cdgC*

Streptomyces spore pigments are frequently aromatic polyketides that are produced by enzymes encoded in the highly conserved *whiE* cluster. In *S. coelicolor*, this cluster comprises an operon of seven genes (*whiE*-ORFI to *whiE*-ORFVII; *sco_5320–sco_5314*) and the divergently transcribed gene *whiE*-ORFVIII (*sco_5321*) (Kelemen *et al*., 1998). In *S. venezuelae*, the homologous cluster is similarly organized and encompasses the genes *vnz_33525* to *vnz_33490*. In the *cdgB* and *cdgC* mutants, *whiE*-ORFI to *whiE*-ORFVII genes were up to 12-fold upregulated (Figure 3d).

Since the *whiE* genes are developmentally regulated and expressed only in spores (Kelemen *et al*., 1998), their upregulation correlates with the morphology of Δ*cdgB* and Δ*cdgC* strains that had already sporulated after 30 h of growth on MYM agar. In contrast, *S. venezuelae* wild type, Δ*rmdA* and Δ*rmdB* were still in the vegetative phase after same incubation period (Figure S2a) and were not expressing the *whiE* genes. *whiE* expression is controlled by the sporulation-specific BldM-WhiI heterodimer (Al-Bassam *et al*., 2014). Since *whiI* is transcribed in an RsiG-(c-di-GMP)-σ^{WhiG}-controlled manner (Gallagher *et al*., 2020), this regulatory circuit is likely responsible for the *whiE* sensitivity to c-di-GMP.

Modulation of c-di-GMP can be an efficient way to manipulate antibiotic production in *Streptomyces* (Makitrynskyy *et al*., 2020). Therefore, we were also interested in identifying antibiotic genes whose expression changed in response to deletion of Δ*cdgB*, Δ*cdgC*, Δ*rmdA*, or Δ*rmdB*. *S. venezuelae* NRRL B-65442 produces the bacteriostatic antibiotic chloramphenicol, a potent inhibitor of bacterial protein biosynthesis. The chloramphenicol biosynthetic gene cluster comprises 17 *cml* genes (*vnz_04400–vnz_04480*). These genes were significantly downregulated in both Δ*cdgB* and Δ*cdgC* strains, but were unaffected in Δ*rmdA* and Δ*rmdB* (Figure 3d). The direct BldD-(c-di-GMP) target gene *bldM* was reported to indirectly repress chloramphenicol genes (Fernandez-Martinez *et al*., 2014) and may represent a link between c-di-GMP signals and chloramphenicol gene expression.

3 | CONCLUSIONS

The DGCs (CdgB and CdgC) and the PDEs (RmdA and RmdB) antagonistically control expression of *ftsZ* via the c-di-GMP-sensors BldD and σ^{WhiG}. Upregulation of *ftsZ* together with other cell division

genes in the DGC mutants is associated with precocious sporulation, while reduced expression of *ftsZ* in the PDE mutants presumably delays sporulation-specific cell division. Thus, c-di-GMP-responsive expression of cell division genes likely contributes to the decision *when* the spores are formed. In addition, expression of chaplin and rodlin genes–encoding the major components of the hydrophobic sheath that covers the aerial hyphae and spores in *Streptomyces*–is controlled by c-di-GMP. Their expression in combination with the transcriptional profile of cell division genes determines *where* the spores are made: on aerial hyphae or out of substrate mycelium. The c-di-GMP enzymes studied here contribute to balanced combination of cell division components and hydrophobins for coordinated progression of the *Streptomyces* life cycle.

4 | MATERIALS AND METHODS

4.1 | Bacterial strains, plasmids and oligonucleotides

All strains, plasmids and oligonucleotides used in this study are listed in Tables S1 and S2 in the supplemental material. *E. coli* strains were grown in LB medium under aerobic conditions. When required, LB was supplemented with 100 μg/ml ampicillin (Amp), 50 μg/ml kanamycin (Kan), 50 μg/ml apramycin (Apr), or 15 μg/ml chloramphenicol (Cam). For hygromycin B (Hyg) –based selection, nutrient agar (NA; Roth) or LB without NaCl (LBon) were used, to which 16 μg/ml or 22 μg/ml, respectively, Hyg was added. *S. venezuelae* strains (Table S2) were grown aerobically at 30°C in liquid Maltose-Yeast Extract-Malt Extract (MYM) medium (Stuttard, 1982) or on MYM agar, both supplemented with trace element solution (Kieser *et al*., 2000). Liquid cultures were inoculated with spores to a final concentration of 10^6 colony-forming-units (CFU) per ml. To study development on MYM agar, 12 μl of 2×10^5 CFU/μl *S. venezuelae* spores were spotted and incubated for the indicated period of time. For hydrophobicity tests, 5 μl of ddH_2O stained with Coomassie Brilliant Blue G-250 were pipetted on top of the colonies that were grown for 43 h. The resulting macrocolonies were photographed using a binocular (Stemi 2000C, Zeiss) coupled with a camera (AxioCAM ICc 3, Zeiss). Digital images were edited using Photoshop CS6 and Illustrator CS6 software (Adobe).

4.2 | Generation of *S. venezuelae* mutant strains

To generate *rmdA*^{ALLEF}, *rmdA*^{AAA}, and *rmdB*^{AAA} mutations on the SV3-B05 and SV2-B03 cosmid, respectively, recombineering using single-strand oligonucleotides (Table S1) in *E. coli* HME68 was performed as described in (Feeney *et al*., 2017). Prior to this, the *kan*-resistance cassette of both cosmids was replaced by *apr-oriT* in *E. coli* BW25113/pIJ790. For that, the *apr-oriT* sequence with *neo*-specific extensions was amplified by PCR from pIJ773 (Table S1 and S2).

Successful mutagenesis was confirmed by PCR and Sanger sequencing and the confirmed mutant cosmids were transformed into *E. coli* ET12567/pUZ8002 for conjugation into *S. venezuelae*, as described in (Bibb *et al*., 2012). Conjugation plates were incubated at room temperature overnight, and then overlayed with Apr. Ex-conjugants were re-streaked once on plates containing Apr and nalidixic acid, and then several times on nonselective medium. The desired mutants arising from a double crossing over were screened for Apr-sensitivity followed by PCR to confirm the desired mutations. PCR products comprising the mutagenized regions were sequenced and the resulting strains were named SVJH29 (*rmdA*^{ALLEF}), SVJH30 (*rmdA*^{AAA}), and SVJH31 (*rmdB*^{AAA}).

4.3 | Complementation of Δ*rmdB*

For complementation analysis of Δ*rmdB* with *rmdB*^{GGAAF}-FLAG, pIJ10170-*rmdB*^{GGAAF}-FLAG was constructed using PCR with pSVJH02 containing *rmdB*-FLAG under the control of the native promoter (Al-Bassam *et al*., 2018) as a template and the PRJH36/PRJH37 primer pair (Table S1). The resulting pSVJH03 plasmid was introduced into the phage integration site Φ_{BT1} in the Δ*rmdB* mutant by conjugation and the strain was named SVJH4.

4.4 | Immunoblot analysis

For detection of FtsZ-YPet, *S. venezuelae* strains expressing *ftsZ-ypet* controlled by the native *ftsZ* promoter on the pSS5 vector (Schlimpert *et al*., 2017) integrated at the Φ_{BT1} phage site, were grown in liquid MYM for 12 h. Two ml were harvested, washed, and homogenized in lysis buffer (20 mM Tris, pH 8, 0.5 mM EDTA and cOmplete protease inhibitor cocktail tablets, EDTA-free (Roche) using a BeadBeater (Biozym; six cycles at 600 m/s; 30 s pulse; 60 s interval). Total protein concentration was determined using the Bradford Assay (Roth) and each sample was adjusted to 1 mg/ml. Fourteen μg total protein were loaded per lane and separated on a 12% of SDS polyacrylamide gel via electrophoresis and transferred to a polyvinylidene difluoride membrane (PVDF, Roth). For immunodetection, anti-GFP antibody was used and bound primary antibody was detected using anti-rabbit IgG-HRP secondary antibody following visualization with the Clarity™ Western ECL Substrate (BioRad) and subsequent detection in a ECL Chemocam Imager (Intas Pharmaceuticals Limited). For semi-quantitative densitometric evaluation of detected FtsZ-YPet, ImageQuant TL software (GE Healthcare Life Sciences) was used to calculate the amount of pixel per band in equal sized areas indicated as arbitrary intensity units (AIU). Signals were normalized to FtsZ-YPet in wild type that were set to 100%.

4.5 | Protein overexpression and purification

Plasmids for overexpression of *cdgE*, *rmdB* (amino acids 244-704), and *rmdA* (amino acids 164-721) were generated using PCR with oligonucleotides listed in Table S1 and either genomic DNA, pSVJH01,

or pSVJH02 (Al-Bassam *et al*., 2018) as templates. *cdgE* and *rmdB* were cloned into pET15b (Novagen), *rmdA* into pMAL-c2 (NEB). *rmdA* $^{G368G;G369G;D370A;E370A;F371F}$ (*rmdA*^{GGAAF}) was created using site directed mutagenesis using the pMAL-c2-*rmdA* plasmid as template. Protein overexpression was induced with IPTG during logarithmic growth of *E. coli* BL21 (DE3) pLysS containing relevant plasmids. 6× His-CdgE and 6× His-RmdB were purified via Ni-NTA chromatography. For MBP-RmdA and MBP-RmdA^{GGAAF} purification, amylose resin (NEB) was applied. For details, please see supplemental material and methods.

4.6 | DGC and PDE assay

Enzymatic activity of RmdA, RmdA^{GGAAF}, RmdB, and CdgE was tested in vitro in PDE and DGC assays, respectively, as described in (Christen *et al*., 2005; Weber *et al*., 2006) with minor modifications. One μM purified protein in cyclase reaction buffer (25 mM Tris HCl, pH 7.5; 250 mM NaCl with 10 mM $MnCl_2$ or $MgCl_2$; 5 mM β-mercaptoethanol; 10% glycerol) was incubated with 4.16 nM [^{32}P]GTP (Hartmann Analytic GmbH) or 2.08 nM [^{32}P]c-di-GMP (Hartmann Analytic GmbH) at 30°C for 60 min. To stop the reaction, 5 μl 0.5 M EDTA, pH 8 was added to an equal volume of reaction mixture followed by heating to 95°C for 5 min. In DGC assays, PleD*, a constitutive active DGC from *C. crescentus* (Paul *et al*., 2004), was added as positive control. In PDE assays, PdeH from *E. coli* (Pesavento *et al*., 2008) served as a positive control. Samples were separated by thin layer chromatography on Polygram CEL 300 PEI cellulose TLC plates (Macherey–Nagel) incubated in 1:1.5 (v/v) saturated $(NH_4)_2SO_4$ and 1.5 M KH_2PO_4; pH 3.6. After drying, the plates were exposed on a Phosphor Imaging Screen (Fuji) which was then scanned using a Typhoon Scanner FLA 7,000 (GE).

4.7 | EMSA

Promotor regions of *cdgA* (172 bp), *cdgC* (205 bp) and *cdgE* (121 bp) were amplified by PCR using specific oligonucleotides (Table S1). Twenty ng of DNA was incubated with 0.6 μM His-tagged BldD, 0.5 μg poly[d(I-C)] (Roche) competitor DNA, and increasing concentrations of c-di-GMP. Each sample was supplemented with 2 μl 10× Bandshift buffer (100 mM Tris-HCl, pH 7.5; 100 mM NaCl; 50 mM DTT; 10 mM EDTA; 10 mM $MgCl_2$; 50% glycerol) and ddH_2O to a total volume of 20 μl. Samples were incubated for 20 min at room temperature and loaded onto a 5% of polyacrylamide gels prepared with TBE buffer. After separation for 1 h at 90 V in 0.5 TBE buffer, DNA was visualized by staining with GelRed (Genaxxon) and exposing to UV light.

4.8 | RNA isolation, RNA-seq and qRT-PCR

Three *S. venezuelae* macrocolonies that were grown for 30 h at 30°C on MYM agar were pooled for one biological replicate and two replicates were used in total for RNA-seq. Cells were resuspended in 200 μl ice-cold stop solution (5% phenol (pH 4.3) in 98% ethanol) and RNA was isolated using the SV Total RNA Isolation Kit (Promega). After elution, RNA was treated with DNaseI (Turbo DNA-free, Ambion). RNA quantity and quality were analyzed using NanoDrop 2000 (Thermo Scientific) and Bioanalyzer 2,100 (Agilent). qRT-PCR was performed using the SensiFAST SYBR No-ROX One-Step Kit (Bioline) and primers listed in Table S1. The RNA-seq libraries were prepared and sequenced in the Illumina NextSeq system by vertis Biotechnologie AG, generating 75 bp single-end reads. The adapter sequences were trimmed from the single-end fastq files using Cutadapt (version 1.18), and low-quality reads were removed.

4.9 | Data analysis

Reads were aligned to the *Streptomyces venezuelae* strain NRRL B-65442 genome (accession no. CP018074) using Bowtie 2, with one mismatch allowed. Samtools (version 1.4.1) was used for downstream coverage calculation. The number of reads per gene was obtained using featureCounts (version 1.5.0-p1). The aligned reads were normalized per kilobase per million (RPKM). Differentially transcribed genes were identified using DESeq2 package in R using p_{adj}-values <0 .05 and log2 fold-change <−1 for (downregulated genes) or >1 (for upregulated genes) as significance thresholds. To generate a heat map of differentially expressed genes, we first grouped the targets into selected functional groups. Then we plotted the RPKM normalized values of those genes if they were differentially transcribed in at least one of the *cdgB*, *cdgC*, *rmdA*, or *rmdB* mutants, using seaborn (version 0.9.0) in Python. To generate Venn diagrams for all the differentially transcribed genes, we used the Venn library (version 0.1.3) in Python. Sequencing data were deposited to the NCBI SRA site under the bioproject accession ID PRJNA608930.

4.10 | Phase-contrast and fluorescence microscopy

Before imaging, samples taken from *S. venezuelae* liquid cultures were washed twice in 1× PBS and 5 μl were pipetted on a thin agarose pad on a microscopy slide. Cells were imaged using the Zeiss Axio Observer Z.1 inverted epifluorescence microscope at 100× magnification and the Axiocam 506 mono. Digital images were organized using ADOBE Photoshop software.

ACKNOWLEDGMENTS

We thank Andreas Latoscha and Mirka E. Wörmann for comments on the manuscript, Susan Schlimpert for the pSS5 plasmid and Heike Bähre for excellent technical assistance with LC-MS/MS analysis. Research in Natalia Tschowri's lab is funded by the DFG Emmy Noether Program (TS 325/1-1) and the DFG Priority Program SPP 1879 (TS 325/2-1 and TS 325/2-2), and in Marie Elliot's lab by the Natural Sciences and Engineering Council of Canada's Discovery

Grant program (RGPIN-2015-04681). Open access funding enabled and organized by Projekt DEAL.

CONFLICT OF INTEREST

The authors declare no competing interests.

AUTHOR CONTRIBUTIONS

N. Tschowri designed the study. Experiments were designed, performed and analyzed by J. Haist, S.A. Neumann, M.M. Al-Bassam, S. Lindenberg, and N. Tschowri. Scientific consultation by M.A. Elliot. The paper was written by N. Tschowri with input from the other authors.

DATA AVAILABILITY STATEMENT

Sequencing data are available on the NCBI SRA site under the bioproject accession ID PRJNA608930.

ORCID

Natalia Tschowri https://orcid.org/0000-0002-4304-1860

REFERENCES

Al-Bassam, M.M., Bibb, M.J., Bush, M.J., Chandra, G. and Buttner, M.J. (2014) Response regulator heterodimer formation controls a key stage in *Streptomyces* development. *PLoS Genetics*, *10*, e1004554.

Al-Bassam, M.M., Haist, J., Neumann, S.A., Lindenberg, S. and Tschowri, N. (2018) Expression patterns, genomic conservation and input into developmental regulation of the GGDEF/EAL/HD-GYP domain proteins in *Streptomyces*. *Frontiers in Microbiology*, *9*, 2524.

Ausmees, N., Wahlstedt, H., Bagchi, S., Elliot, M.A., Buttner, M.J. and Flärdh, K. (2007) SmeA, a small membrane protein with multiple functions in *Streptomyces* sporulation including targeting of a SpoIIIE/FtsK-like protein to cell division septa. *Molecular Microbiology*, *65*, 1458–1473.

Bibb, M.J., Domonkos, A., Chandra, G. and Buttner, M.J. (2012) Expression of the chaplin and rodlin hydrophobic sheath proteins in *Streptomyces venezuelae* is controlled by sigma(BldN) and a cognate anti-sigma factor, RsbN. *Molecular Microbiology*, *84*, 1033–1049.

Bush, M.J., Bibb, M.J., Chandra, G., Findlay, K.C. and Buttner, M.J. (2013) Genes required for aerial growth, cell division, and chromosome segregation are targets of WhiA before sporulation in *Streptomyces venezuelae*. *mBio*, *4*(5), e00684-13. https://doi.org/10.1128/mBio.00684-13.

Bush, M.J., Chandra, G., Al-Bassam, M.M., Findlay, K.C. and Buttner, M.J. (2019) BldC delays entry into development to produce a sustained period of vegetative growth in *Streptomyces venezuelae*. *mBio*, *10*(1), e02812-18. https://doi.org/10.1128/mBio.02812-18

Bush, M.J., Tschowri, N., Schlimpert, S., Flärdh, K. and Buttner, M.J. (2015) c-di-GMP signalling and the regulation of developmental transitions in streptomycetes. *Nature Reviews Microbiology*, *13*, 749–760.

Christen, M., Christen, B., Folcher, M., Schauerte, A. and Jenal, U. (2005) Identification and characterization of a cyclic di-GMP-specific phosphodiesterase and its allosteric control by GTP. *The Journal of Biological Chemistry*, *280*, 30829–30837.

Claessen, D., Rink, R., de Jong, W., Siebring, J., de Vreugd, P., Boersma, F.G., *et al.* (2003) A novel class of secreted hydrophobic proteins is involved in aerial hyphae formation in *Streptomyces coelicolor* by forming amyloid-like fibrils. *Genes & Development*, *17*, 1714–1726.

Claessen, D., Wosten, H.A., van Keulen, G., Faber, O.G., Alves, A.M., Meijer, W.G., *et al.* (2002) Two novel homologous proteins of *Streptomyces coelicolor* and *Streptomyces lividans* are involved in the formation of the rodlet layer and mediate attachment to a hydrophobic surface. *Molecular Microbiology*, *44*, 1483–1492.

den Hengst, C.D., Tran, N.T., Bibb, M.J., Chandra, G., Leskiw, B.K. and Buttner, M.J. (2010) Genes essential for morphological development and antibiotic production in *Streptomyces coelicolor* are targets of BldD during vegetative growth. *Molecular Microbiology*, *78*, 361–379.

Di Berardo, C., Capstick, D.S., Bibb, M.J., Findlay, K.C., Buttner, M.J. and Elliot, M.A. (2008) Function and redundancy of the chaplin cell surface proteins in aerial hypha formation, rodlet assembly, and viability in *Streptomyces coelicolor*. *Journal of Bacteriology*, *190*, 5879–5889.

Elliot, M.A., Bibb, M.J., Buttner, M.J. and Leskiw, B.K. (2001) BldD is a direct regulator of key developmental genes in *Streptomyces coelicolor* A3(2). *Molecular Microbiology*, *40*, 257–269.

Elliot, M.A., Karoonuthaisiri, N., Huang, J., Bibb, M.J., Cohen, S.N., Kao, C.M., *et al.* (2003) The chaplins: a family of hydrophobic cell-surface proteins involved in aerial mycelium formation in *Streptomyces coelicolor*. *Genes & Development*, *17*, 1727–1740.

Feeney, M.A., Chandra, G., Findlay, K.C., Paget, M.S.B. and Buttner, M.J. (2017) Translational control of the SigR-directed oxidative stress response in streptomyces via IF3-mediated repression of a noncanonical GTC start codon. *mBio*, *8*(3), e00815-17. https://doi.org/10.1128/mBio.00815-17

Fernandez-Martinez, L.T., Borsetto, C., Gomez-Escribano, J.P., Bibb, M.J., Al-Bassam, M.M., Chandra, G., *et al.* (2014) New insights into chloramphenicol biosynthesis in *Streptomyces venezuelae* ATCC 10712. *Antimicrobial Agents and Chemotherapy*, *58*, 7441–7450.

Flärdh, K., Leibovitz, E., Buttner, M.J. and Chater, K.F. (2000) Generation of a non-sporulating strain of *Streptomyces coelicolor* A3(2) by the manipulation of a developmentally controlled *ftsZ* promoter. *Molecular Microbiology*, *38*, 737–749.

Gallagher, K.A., Schumacher, M.A., Bush, M.J., Bibb, M.J., Chandra, G., Holmes, N.A., *et al.* (2020) c-di-GMP arms an anti-sigma to control progression of multicellular differentiation in *Streptomyces*. *Molecular Cell*, *77*(586–599), e586.

Haeusser, D.P. and Margolin, W. (2016) Splitsville: structural and functional insights into the dynamic bacterial Z ring. *Nature Reviews Microbiology*, *14*, 305–319.

Heichlinger, A., Ammelburg, M., Kleinschnitz, E.M., Latus, A., Maldener, I., Flärdh, K., *et al.* (2011) The MreB-like protein Mbl of *Streptomyces coelicolor* A3(2) depends on MreB for proper localization and contributes to spore wall synthesis. *Journal of Bacteriology*, *193*, 1533–1542.

Hengge, R. (2009) Principles of c-di-GMP signalling in bacteria. *Nature Reviews Microbiology*, *7*, 263–273.

Hull, T.D., Ryu, M.H., Sullivan, M.J., Johnson, R.C., Klena, N.T., Geiger, R.M., *et al.* (2012) Cyclic di-GMP phosphodiesterases RmdA and RmdB are involved in regulating colony morphology and development in *Streptomyces coelicolor*. *Journal of Bacteriology*, *194*, 4642–4651.

Jakimowicz, D. and van Wezel, G.P. (2012) Cell division and DNA segregation in *Streptomyces*: how to build a septum in the middle of nowhere? *Molecular Microbiology*, *85*, 393–404.

Jenal, U., Reinders, A. and Lori, C. (2017) Cyclic di-GMP: second messenger extraordinaire. *Nature Reviews Microbiology*, *15*, 271–284.

Kelemen, G.H., Brian, P., Flärdh, K., Chamberlin, L., Chater, K.F. and Buttner, M.J. (1998) Developmental regulation of transcription of *whiE*, a locus specifying the polyketide spore pigment in *Streptomyces coelicolor* A3 (2). *Journal of Bacteriology*, *180*, 2515–2521.

Kieser, T., Bibb, M.J., Buttner, M.J., Chater, K.F. and Hopwood, D.A. (2000) *Practical Streptomyces Genetics*. Norwich: The John Innes Foundation.

Kleinschnitz, E.M., Heichlinger, A., Schirner, K., Winkler, J., Latus, A., Maldener, I., *et al.* (2011) Proteins encoded by the mre gene cluster in *Streptomyces coelicolor* A3(2) cooperate in spore wall synthesis. *Molecular Microbiology*, *79*, 1367–1379.

Latoscha, A., Wormann, M.E. and Tschowri, N. (2019) Nucleotide second messengers in *Streptomyces*. *Microbiology*, *165*, 1153–1165.

Lim, B., Beyhan, S., Meir, J. and Yildiz, F.H. (2006) Cyclic-di GMP signal transduction systems in *Vibrio cholerae*: modulation of rugosity and biofilm formation. *Molecular Microbiology*, *60*, 331–348.

Lindenberg, S., Klauck, G., Pesavento, C., Klauck, E. and Hengge, R. (2013) The EAL domain protein YciR acts as a trigger enzyme in a c-di-GMP signalling cascade in *E. coli* biofilm control. *The EMBO Journal*, *32*, 2001–2014.

Makitrynskyy, R., Tsypik, O., Nuzzo, D., Paululat, T., Zechel, D.L. and Bechthold, A. (2020) Secondary nucleotide messenger c-di-GMP exerts a global control on natural product biosynthesis in streptomycetes. *Nucleic Acids Research*, *48*, 1583–1598.

Noens, E.E., Mersinias, V., Traag, B.A., Smith, C.P., Koerten, H.K. and van Wezel, G.P. (2005) SsgA-like proteins determine the fate of peptidoglycan during sporulation of *Streptomyces coelicolor*. *Molecular Microbiology*, *58*, 929–944.

Paul, R., Weiser, S., Amiot, N.C., Chan, C., Schirmer, T., Giese, B., *et al*. (2004) Cell cycle-dependent dynamic localization of a bacterial response regulator with a novel di-guanylate cyclase output domain. *Genes & Development*, *18*, 715–727.

Pesavento, C., Becker, G., Sommerfeldt, N., Possling, A., Tschowri, N., Mehlis, A., *et al*. (2008) Inverse regulatory coordination of motility and curli-mediated adhesion in *Escherichia coli*. *Genes & Development*, *22*, 2434–2446.

Richter, A.M., Possling, A., Malysheva, N., Yousef, K.P., Herbst, S., von Kleist, M., *et al*. (2020) Local c-di-GMP signaling in the control of synthesis of the *E. coli* biofilm exopolysaccharide pEtN-cellulose. *Journal of Molecular Biology*, *432*(16), 4576–4595. https://doi.org/10.1016/j.jmb.2020.06.006

Römling, U., Galperin, M.Y., & Gomelsky, M. (2013). Cyclic di-GMP: the first 25 years of a universal bacterial second messenger. *Microbiology and Molecular Biology Reviews: MMBR*, *77*, 1–52.

Sarenko, O., Klauck, G., Wilke, F.M., Pfiffer, V., Richter, A.M., Herbst, S., *et al*. (2017) More than enzymes that make or break cyclic Di-GMP-local signaling in the interactome of GGDEF/EAL domain proteins of *Escherichia coli*. *mBio*, *8*(5), e01639-17. https://doi.org/10.1128/mBio.01639-17

Schlimpert, S., Wasserstrom, S., Chandra, G., Bibb, M.J., Findlay, K.C., Flärdh, K., *et al*. (2017) Two dynamin-like proteins stabilize FtsZ rings during *Streptomyces* sporulation. *Proceedings of the National Academy of Sciences of the United States of America*, *114*, E6176–E6183.

Schmidt, A.J., Ryjenkov, D.A. and Gomelsky, M. (2005) The ubiquitous protein domain EAL is a cyclic diguanylate-specific phosphodiesterase: enzymatically active and inactive EAL domains. *Journal of Bacteriology*, *187*, 4774–4781.

Schumacher, M.A., Bush, M.J., Bibb, M.J., Ramos-Leon, F., Chandra, G., Zeng, W., *et al*. (2018a) The crystal structure of the RsbN-sigmaBldN complex from *Streptomyces venezuelae* defines a new structural class of anti-sigma factor. *Nucleic Acids Research*, *46*, 7467–7468.

Schumacher, M.A., den Hengst, C.D., Bush, M.J., Le, T.B.K., Tran, N.T., Chandra, G., *et al*. (2018b) The MerR-like protein BldC binds DNA direct repeats as cooperative multimers to regulate *Streptomyces* development. *Nature Communications*, *9*, 1139.

Schumacher, M.A., Zeng, W., Findlay, K.C., Buttner, M.J., Brennan, R.G. and Tschowri, N. (2017) The *Streptomyces* master regulator BldD binds c-di-GMP sequentially to create a functional $BldD_2$-$(c\text{-}di\text{-}GMP)_4$ complex. *Nucleic Acids Research*, *45*, 6923–6933.

Som, N.F., Heine, D., Holmes, N.A., Munnoch, J.T., Chandra, G., Seipke, R.F., *et al*. (2017) The conserved actinobacterial two-component system MtrAB coordinates chloramphenicol production with sporulation in *Streptomyces venezuelae* NRRL B-65442. *Frontiers in Microbiology*, *8*, 1145.

Stuttard, C. (1982) Temperate phages of *Streptomyces venezuelae*: lysogeny and host specificity shown by phages SV1 and SV2. *Microbiology*, *128*, 115–121.

Tran, N.T., Den Hengst, C.D., Gomez-Escribano, J.P. and Buttner, M.J. (2011) Identification and characterization of CdgB, a diguanylate cyclase involved in developmental processes in *Streptomyces coelicolor*. *Journal of Bacteriology*, *193*, 3100–3108.

Tschowri, N., Schumacher, M.A., Schlimpert, S., Chinnam, N.B., Findlay, K.C., Brennan, R.G., *et al*. (2014) Tetrameric c-di-GMP mediates effective transcription factor dimerization to control *Streptomyces* development. *Cell*, *158*, 1136–1147.

Weber, H., Pesavento, C., Possling, A., Tischendorf, G. and Hengge, R. (2006) Cyclic-di-GMP-mediated signalling within the σ^S network of *Escherichia coli*. *Molecular Microbiology*, *62*, 1014–1034.

Willemse, J., Borst, J.W., de Waal, E., Bisseling, T. and van Wezel, G.P. (2011) Positive control of cell division: FtsZ is recruited by SsgB during sporulation of *Streptomyces*. *Genes & Development*, *25*, 89–99.

Willey, J., Santamaria, R., Guijarro, J., Geistlich, M. and Losick, R. (1991) Extracellular complementation of a developmental mutation implicates a small sporulation protein in aerial mycelium formation by *S. coelicolor*. *Cell*, *65*, 641–650.

Yan, H., Lu, X., Sun, D., Zhuang, S., Chen, Q., Chen, Z., *et al*. (2020) BldD, a master developmental repressor, activates antibiotic production in two *Streptomyces* species. *Molecular Microbiology*, *113*, 123–142.

SUPPORTING INFORMATION

Additional Supporting Information may be found online in the Supporting Information section.

How to cite this article: Haist J, Neumann SA, Al-Bassam MM, Lindenberg S, Elliot MA, Tschowri N. Specialized and shared functions of diguanylate cyclases and phosphodiesterases in *Streptomyces* development. *Mol Microbiol*. 2020;00:1–15. https://doi.org/10.1111/mmi.14581